ACTA ABP BIOCHIMICA POLONICA

Vol. 70, No 3/2023
721–727
https://doi.org/10.18388/abp.2020_6242

Regular paper

MicroRNA-411-3p motivates methotrexate's cellular uptake and cytotoxicity *via* targeting Yin-yang 1 in leukemia cells

HuiJing Sun[1#], ShuGuang Zhou[1#], ZhouSheng Yang[1], MingYu Meng[1], Yan Dai[2], XinYe Li[2] and XiaoYu Chen[1]✉

[1]Department of Pharmacy, The People's Hospital of Guangxi Zhuang Autonomous Region, Nanning City, Guangxi Zhuang Autonomous Region, 530021, China; [2]Department of Paediatrics, The People's Hospital of Guangxi Zhuang Autonomous Region, Nanning City, Guangxi Zhuang Autonomous Region, 530021, China

This study aimed to figure out how microRNA (miR)-411-3p's impacts on methotrexate (MTX)'s cellular uptake and cytotoxicity in acute lymphoblastic leukaemia (ALL) CEM-C1 cells by targeting Yin-yang 1 (YY1). miR-411-3p and YY1 were detected by RT-qPCR or Western blot. Intracellular MTX concentration was measured by enzyme-linked immunosorbent assay. Cell viability and apoptosis were evaluated by CCK-8, clonal formation assay, and flow cytometry. Verification of miR-411-3p and YY1's targeting link was manifested. It came out that miR-411-3p mimic or si-YY1 elevated intracellular MTX, MTX-induced cytotoxicity and apoptosis rate in CEM-C1. However, the inverse results were noticed in cells introduced with miR-411-3p inhibitor or oe-YY1. Meanwhile, it was found that cell relative luciferase activity was reduced after co-transfection of miR-411-3p mimic with YY1-WT, indicating that miR-411-3p targeted YY1. Elevation of YY1 could turn around elevating miR-411-3p's impacts on MTX's cellular uptake and cytotoxicity in CEM-C1 cells. These findings convey that miR-411-3p motivated MTX's cellular uptake and cytotoxic impacts via targeting YY1 in leukemia cells. This study is helpful for learning about the mechanisms underlying MTX responses in ALL patients.

Keywords: MicroRNA-411-3p, Yin-yang 1, methotrexate, acute lymphoblastic leukemia

Received: 01 March, 2023; revised: 19 December, 2022; accepted: 18 April, 2023; available on-line: 19 September, 2023

✉e-mail: cxiaoyuchina@hotmail.com
#These authors contributed equally to this work.
Acknowledgements of Financial Support: Guangxi Zhuang Autonomous Region Self-funded by Health Commission of Guangxi Zhuang Autonomous Region, (No. Z20190278).
Abbreviations: ALL, Acute lymphoblastic leukaemia; MTX, methotrexate; YY1, Yin-yang 1

INTRODUCTION

Acute lymphoblastic leukaemia (ALL) is an extremely common malignant tumor, which frequently shows up in children, taking up about 80% of ALL cases, and occasionally takes place in adults (Liang *et al.,* 2021). ALL is featured by malignant transformation and proliferation of T- or B-cell progenitors which invade blood, bone marrow, and extramedullary sites, thereby preventing normal blood cell production (Ranjbar *et al.,* 2019). Methotrexate (MTX) is a chemotherapeutic drug for ALL and has been applied to cure leukemia and lymphoma patients (Woźniak *et al.,* 2021). Although most patients are available to achieve long-term disease-free survival *via* standardized treatments, including MTX, some ALL treatments for children are still ineffective, and drug resistance is a vital reason for this phenomenon (Jaramillo *et al.,* 2019). Therefore, discovering approaches to suppress chemotherapy resistance in ALL patients is crucial for ALL cure.

MTX is a folate antagonist, whose action is extremely complicated, involving some transporters determining intracellular drug levels and active MTX polyglutamate and some metabolic enzymes (Gervasini *et al.,* 2017). MTX enters cells by passive diffusion via the solute carrier 19A1 transporter (RFC1) (Ando *et al.,* 2013), while the drug is pumped out by some membrane efflux transporters of the ATP-binding cassette family (Aberuyi *et al.,* 2021). MTX is converted into active polyglutamate form (MTX polyglutamate, MTXPG) by folate polyglutamate synthase intracellularly (De Beaumais *et al.,* 2012). MTX and MTXPG inhibit thymidine synthesis by targeting dihydrofolate reductase and thymidine synthase (Rushworth *et al.,* 2015), thereby impairing DNA and RNA synthesis and leading to cell death (Oosterom *et al.,* 2018). In conclusion, the accumulation of MTX and its active metabolite methotrexate polyglutamate (MTXPG) in all cells is an important determinant of its anti-leukemia effect (Panetta *et al.,* 2010).

MicroRNAs (miRNAs), a cluster of endogenous single-stranded non-coding RNAs, modulate gene expression (Lin *et al.,* 2021). Much evidence illustrates that miRNAs participate in almost all biological processes, including drug resistance (Xian *et al.,* 2019; Naghizadeh *et al.,* 2020; Wei *et al.,* 2021). Genetic variation in MTX transporter genes has been reported to be implicated in toxicity, and these transporters are controlled by miRNAs (Iparraguirre *et al.,* 2016). Wang SM (Wang *et al.,* 2017). confirm that two miRNA-binding site polymorphisms (rs3737966 G>A and rs35134728 DEL/TTC) in the 3'-UTR of 5,10-methylenetetrahydrofolate reductase were linked with serum MTX concentrations. Xu Wen (Xu *et al.,* 2018). discovered that miR-29 family restrained MTX resistance but motivated apoptosis by targeting COL3A1 and MCL1 in osteosarcoma. MiR-411-3p, a newly studied miRNA, has been discovered to be aberrantly expressed in some human cancers (Huang *et al.,* 2021; Wang *et al.,* 2019; Wang *et al.,* 2020). However, no studies have been conducted to clarify its role in MTX resistance. In the research, the main focus was on miR-411-3p's function in controlling Yin-yang 1 (YY1) and its impact on ALL CEM-C1 cell uptake and MTX cytotoxicity.

MATERIALS AND METHODS

Cell culture

Growth of human ALL CEM-C1 cells was in Roswell Park Memorial Institute – 1640 medium replenished with 10% fetal bovine serum (Gibco, Grand Island, NY, USA), 100 U/ml penicillin, and 100 U/ml streptomycin (Beyotime Biotechnology, Shanghai, China). CEM-C1 cells were purchased from the Cell Bank of the Chinese Academy of Sciences (Shanghai, China).

Cell transfection

Synthesis of miR-411-3p mimic/inhibitor, mimic/inhibitor negative control (NC), si-YY1/-NC, and oe-YY1/-NC was done by Invitrogen. Oligonucleotides or plasmids (8 μmol/ml) were transfected into CEM-C1 cells based on Lipofectamine 2000 reagent (Invitrogen; Thermo Fisher Scientific). After transfection, cells were treated with different concentrations of MTX (10, 20 and 40 ng/ml).

Intracellular MTX Concentration Determination

Cells were dispersed in 96-well plates at 5.0×10^5 cells per well prior to transfection and MTX treatment. Quantification of intracellular MTX was done using human methotrexate, MTX ELISA kit (HB1386-Hu, Shanghai Hengyuan Biotechnology Co., LTD). Absorbance at 450 nm was recorded on a microplate reader (ELX800, BioTek Instruments, Inc.) and MTX concentrations were calculated.

Cell proliferation assay

Cell proliferation assays were conducted using the Cell Counting Kit-8 (CCK-8; Beyotime Institute of Biotechnology, Inc.). CEM-C1 cells were combined with CCK-8 solution (10 μL) in each well. Next, 4-h cell incubation was conducted, followed by measurement of optical density (OD) value at 450 nm on a microplate reader (ELX800, BioTek Instruments, Inc.). Proliferation rate: {[(ODcontrol-ODblank)-(ODtreated-ODblank)]/(ODcontrol-ODblank)} 100%.

Colony formation assay

Treatment of transfected CEM-C1 cells was done with different concentrations of MTX (10, 20 and 40 ng/ml). The cells were then transferred to a 6-well plate (1×10^3 cells/well) and supplemented with RPMI-1640 medium containing 10% fetal bovine serum at 37°C. After 14 days, the cells were fixed with formaldehyde and stained with 0.1% crystal violet solution (Sigma Aldrich) at 25°C for 15 min and counted under a CKX41 microscope (Olympus).

Apoptosis assay

Annexin V-fluorescein isothiocyanate Apoptosis Detection Kit (BD, USA) was applied to detect apoptosis. In brief, cells were stained with 10 μl Annexin V and 5 μl propidium iodide for 15 min. Then, quantitative analysis was performed using BD FACSCalibur™ (BD, USA).

Reverse transcription quantitative polymerase chain reaction (RT-qPCR)

Total RNA's extraction was conducted using the miRNeasy extraction kit (Qiagen, Valencia, CA, USA). MiR-411-3p's quantification was conducted using the Hairpin-it miRNA qPCR quantification kit (GenePharma, Shanghai, China) with U6 as a loading control. Detection of YY1 was implemented using Power SYBR Green PCR Master Mix (Applied Biosystems) with glyceraldehyde-3-phosphate dehydrogenase (GAPDH) as internal control, and all PCR reactions were conducted on a 7500 Fast Real-Time PCR Systems (Applied Biosystems, CA, USA). All primer sequences were manifested in Table 1. Calculation of miR-411-3p or YY1 was implemented using the $2^{-\Delta\Delta CT}$ method (Wu *et al.,* 2020).

Table 1. RT-qPCR primers

Genes	Primer sequence (5′-3′)
MiR-411-3p	F: CCGAGTATGTAACACGGTC
	R: TATGTAACACGGTCCACTAACC
YY1	F: AAAACGACACCAACTGGTTCATAC
	R: AAGTCCAGTGAAAAGCGTTTCC
Bcl-2	F: ATCCAGGACAACGGAGGCTG
	R: CAGATAGGCACCCAGGGTGA
Bax	F: GATCGAGCAGGGCGAATG
	R: CATCTCAGCTGCCACTCG
U6	F: CTCGCTTCGGCAGCACA
	R: AACGCTTCACGAATTTGCGT
GAPDH	F: CACCCACTCCTCCACCTTTG
	R: CCACCACCCTGTTGCTGTAG

Western blot

Isolation of total protein was done using mammalian protein extraction reagents (Thermo Fisher Scientific, Inc.) and 1% protease inhibitor cocktail (Merck KGaA, Darmstadt, Germany). The Bicinchoninic acid assay method (Thermo Fisher Scientific, Inc.) was applied for determining the protein concentration. 10 μg protein separated by 1% sodium dodecyl sulfate-polyacrylamide gel electrophoresis was electro-blotted onto polyvinylidene fluoride membranes (Millipore, Bedford, MA, USA), followed by blocking with 7% skim milk and incubation with primary antibody and horseradish peroxidase-conjugated secondary antibody (ab6721; 1: 2000; Abcam). Primary antibodies applied in this study included: YY1 (sc-7341; 1: 1000; Santa Cruz Biotechnology) and GAPDH (ab8245; 1: 1000; Abcam). Detection of proteins was done by enhanced chemiluminescence (Thermo Fisher Scientific, Inc.) (Liu *et al.,* 2019).

The luciferase activity assay

Construction of the luciferase reporter gene plasmids (Promega, USA) covering the 3'-UTR of YY1 with forecast miR-411-3p target sites (Wild-type) or the mutated sites of 3'UTR of YY1 (Mutant) was implemented. Transient co-transfection of CEM-C1 cells was then done with reporters and miR-411-3p mimic or mimic NC. Detection of Firefly and renilla luciferase activities was conducted using a dual-luciferase reporter assay system (Promega) (Liu *et al.,* 2020).

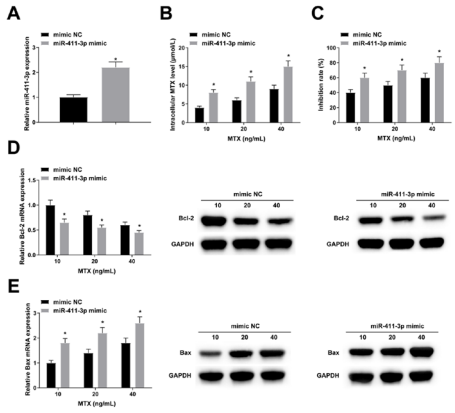

Figure 1. Elevating miR-411-3p motivates MTX's cellular uptake and cytotoxic influences.
(**A**) RT-qPCR detection of miR-411-3p; (**B**) ELISA detection of intracellular MTX concentration; (**C**) CCK-8 detection of cell viability; (**D/E**) RT-qPCR and Western blot detection of Bcl-2 and Bax; the values were clarified as mean ± S.D. (N=3); *vs*. the mimic NC, $P<0.05$.

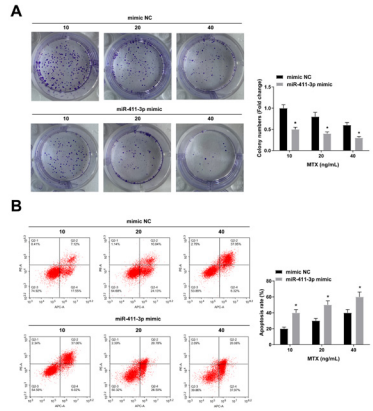

Figure 2. Elevating miR-411-3p motivates MTX's cellular uptake and cytotoxic influences.
(**A**) Clone formation assay detection of cell proliferation; (**B**) Flow cytometry detection of cell apoptosis; The data in the figures were all measurement data, and the values were clarified as mean ± S.D. (N=3); *vs*. the mimic NC, $P<0.05$.

2RNA immunoprecipitation (RIP)

Cell lysates were collected. Incubation of the supernatant from cell lysates was implemented with human anti-Ago2 antibody (SCBT, Santa Cruz, CA, USA) or mouse Immunoglobulin G (SCBT, Santa Cruz). Detachment of proteins was done using Proteinase K buffer and the quantitative real time PCR examined co-precipitated RNAs.

2Statistical analysis

Data were presented as mean ± standard deviation (S.D.) unless otherwise noted. Two groups' comparisons were implemented using the unpaired two-tailed Student's *t*-test. Application of Graphpad Prism software version 4.0 was for all statistical analyses. $P<0.05$ emphasized obvious statistical meaning.

RESULTS

Elevating miR-411-3p motivates MTX's cellular uptake and cytotoxic influences

CEM/C1 cells were transfected with miR-411-3p mimic or mimic NC. miR-411-3p was elevated after transfection of miR-411-3p mimic (Fig. 1A). CEM/C1 cells were treated with disparate concentrations of MTX (10, 20 and 40 ng/ml). Detection of the intracellular MTX concentration was conducted, and the results displayed that the intracellular MTX was elevated in CEM/CI cells introduced with miR-411-3p mimic (Fig. 1B). The cell growth was tested. The results illustrated that after incubation with different concentrations of MTX, elevating miR-411-3p resulted in a clear augmentation in the repression rate of CEM/CI cells (Fig. 1C) and a memorable decline in the number of colonies (Fig. 2A). Considering that apoptosis is a mechanism by which MTX exerts its antitumor effect, the latent function of miR-411-3p in MTX-induced apoptosis in CEM/CI cells was then figured out. It turned out that the apoptosis index of CEM/CI cells in the miR-411-3p mimic introduced with different concentrations of MTX was elevated at all MTX concentrations (Fig. 2B). Moreover, after incubation with different concentrations of MTX, enhancing miR-411-3p could restrain Bcl-2 but accelerate Bax (Fig. 1D–E). These results suggest that elevating miR-411-3p restrains CEM/C1 cell growth by motivating MTX's cellular uptake and cytotoxic influences.

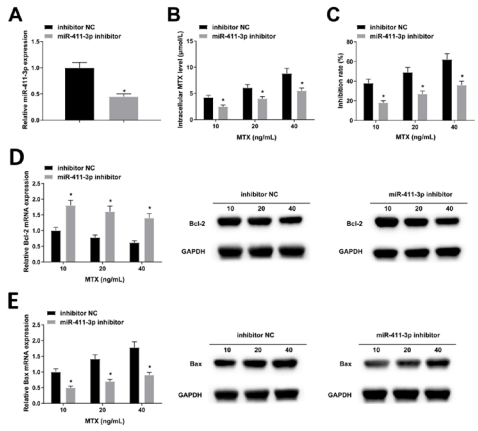

Figure 3. Depressing miR-411-3p restrains the cellular uptake and cytotoxic effects of MTX.
(**A**) RT-qPCR detection of miR-411-3p; (**B**) ELISA detection of intracellular MTX concentration; (**C**) CCK-8 detection of cell viability; (**D/E**) RT-qPCR and Western blot detection of Bcl-2 and Bax; the values were clarified as mean ± S.D. (N=3); *vs*. the inhibitor NC, $P<0.05$.

Depressing miR-411-3p restrains MTX's cellular uptake and cytotoxic influences

To further testify miR-411-3p's function, miR-411-3p inhibitor or inhibitor NC was transfected into CEM/C1 cells, and the successful transfection was verified (Fig. 3A). It turned out that intracellular MTX was clearly reduced in CEM/CI cells introduced with miR-411-3p inhibitor (Fig. 3B). It came out after incubation with different concentrations of MTX, that depressing miR-411-3p resulted in a clear decline of the repression rate of CEM/CI cells (Fig. 3C) and a distinct elevation in the number of colonies (Fig. 4A). Meanwhile, CEM/CI cells' apoptosis index after depressing miR-411-3p was declined at all MTX concentrations (Fig. 4B). Moreover, after incubation with different concentrations of MTX, depressing miR-411-3p could motivate Bcl-2 but restrain Bax (Fig. 3D/E). Taken together, repressing miR-411-3p

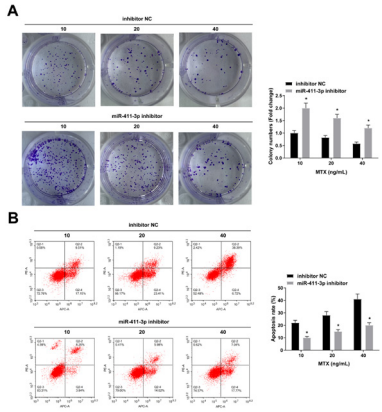

Figure 4. Depressing miR-411-3p restrains the cellular uptake and cytotoxic effects of MTX.
(**A**) Clone formation assay detection of cell proliferation; (**B**) Flow cytometry detection of cell apoptosis; the values were clarified as mean ± S.D. (N=3); *vs. the inhibitor NC, *P*<0.05.

motivates CEM/C1 cell growth by refraining MTX's cellular uptake and cytotoxic influences.

MiR-411-3p targets YY1

For further understand miR-411-3p's possible downstream mechanism, Starbase database was applied to forecast that miR-411-3p had a binding site with YY1 (Fig. 5A). YY1 was clearly reduced after elevating miR-411-3p, while depressive miR-411-3p could motivate YY1 (Fig. 5B). Then for further verification of their targeting link, the luciferase activity assay was conducted. Results illustrating co-transfection of YY1-WT with miR-411-3p mimic showed a clear decrease in cell luciferase activity (Fig. 5C). Moreover, miR-411-3p and YY1 were apparently abundant in Ago2 immuno-precipitates (Fig. 5D). These results clarify that miR-411-3p targets YY1.

Depressing YY1 motivates MTX's cellular uptake and cytotoxic influences

To figure out YY1's impact on MTX's cellular uptake and cytotoxicity in CEM/C1 cells, si-YY1/NC was

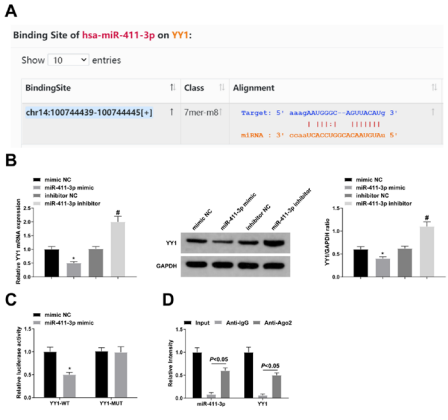

Figure 5. MiR-411-3p negatively modulates YY1.
(**A**) The binding site of miR-411-3p and YY1 predicted by Starbase database; (**B**) RT-qPCR and Western blot detection of YY1; (**C**) The targeting link between miR-411-3p and YY1 verified by the luciferase activity assay; (**D**) RIP experiment verification of the targeting link between miR-411-3p and YY1; the values were clarified as mean ± S.D. (N=3); *vs. the mimic NC, *P*<0.05; #vs. the inhibitor NC, *P*<0.05.

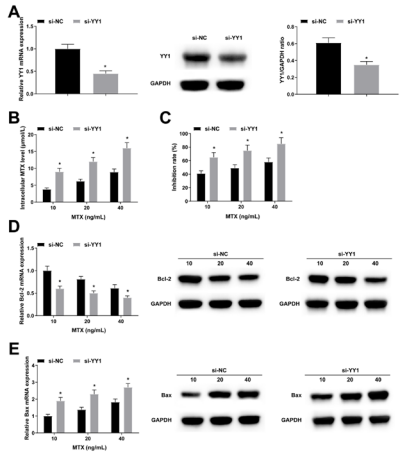

Figure 6. Depressing YY1 motivates the cellular uptake and cytotoxic effects of MTX.
(**A**) RT-qPCR and Western blot detection of YY1; (**B**) ELISA detection of intracellular MTX concentration; (**C**) CCK-8 detection of cell viability; (**D/E**) RT-qPCR and Western blot detection of Bcl-2 and Bax; the values were clarified as mean ± S.D. (N=3); *vs. the si-NC, *P*<0.05.

transfected into CEM/C1 cells (Fig. 6A). It turned out that intracellular MTX was clearly elevated in CEM/CI cells transfected with si-YY1 (Fig. 6B). It came out that after incubation with different concentrations of MTX, repressing YY1 resulted in a clear elevation in the inhibition rate of CEM/CI cells (Fig. 6C) and a distinct decline in the number of colonies (Fig. 7A). It turned out that the apoptosis index of CEM/CI cells in the si-YY1 treated with different concentrations of MTX was elevated at all MTX concentrations (Fig. 7B). Moreover, after incubation with different concentrations of MTX, depressing YY1 could restrain Bcl-2 but motivate Bax (Fig. 6D/E). The above results illustrate that repressive YY1 can accelerate MTX's cellular uptake and cytotoxicity, thereby refraining CEM/C1 cell growth.

Enhancing YY1 restrains MTX's cellular uptake and cytotoxic influences

To further testify YY1's role, it was transfected oe-YY1/NC into CEM/C1 cells and successful transfection was verified (Fig. 8A). It turned out that intracellular

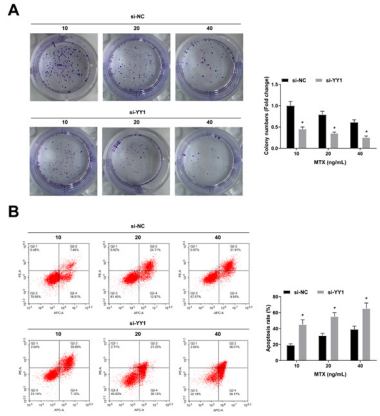

Figure 7. Depressing YY1 motivates the cellular uptake and cytotoxic effects of MTX.
(**A**) Clone formation assay detection of cell proliferation; (**B**) Flow cytometry detection of cell apoptosis; the values were clarified as mean ± S.D. (N=3); *vs. the si-NC, *P*<0.05.

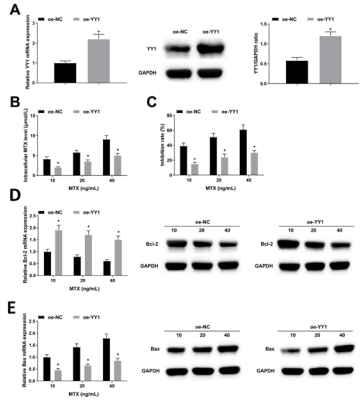

Figure 8. Enhancing YY1 restrains the cellular uptake and cytotoxic effects of MTX.
(**A**) RT-qPCR and Western blot detection of YY1; (**B**) ELISA detection of intracellular MTX concentration; (**C**) CCK-8 detection of cell viability; (**D/E**) RT-qPCR and Western blot detection of Bcl-2 and Bax; the values were clarified as mean ± S.D. (N=3); *vs. the oe-NC, $P<0.05$.

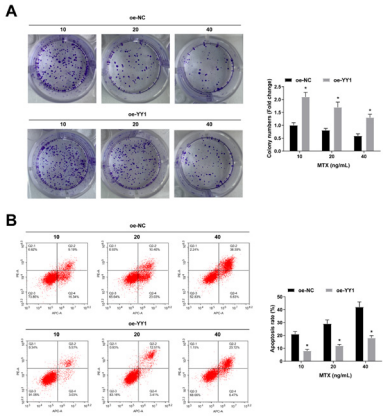

Figure 9. Enhancing YY1 restrains the cellular uptake and cytotoxic effects of MTX.
(**A**) Clone formation assay detection of cell proliferation; (**B**) Flow cytometry detection of cell apoptosis; The data in the figures were all measurement data, and the values were clarified as mean ± S.D. (N=3); *vs. the oe-NC, $P<0.05$.

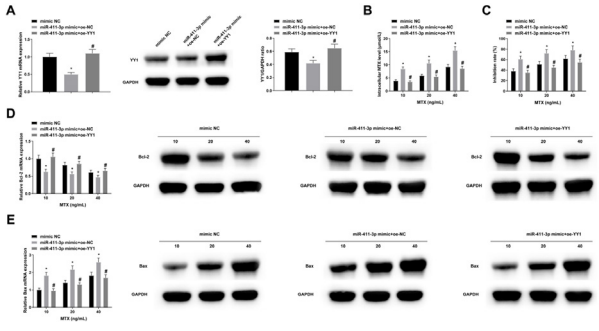

Figure 10. Elevation of YY1 could turn around elevating miR-411-3p's impacts on MTX cellular uptake and cytotoxicity in CEM-C1 cells.
(**A**) RT-qPCR and Western blot verification of successful transfection; (**B**) ELISA detection of intracellular MTX concentration; (**C**) CCK-8 detection of cell viability; (**D/E**) RT-qPCR and Western blot detection of apoptosis-linked genes (Bcl-2 and Bax); The data in the figures were all measurement data, and the values were clarified as mean ± S.D. (N=3); *vs. the mimic NC group, $P<0.05$; #vs. the miR-411-3p mimic+oe-NC, $P<0.05$.

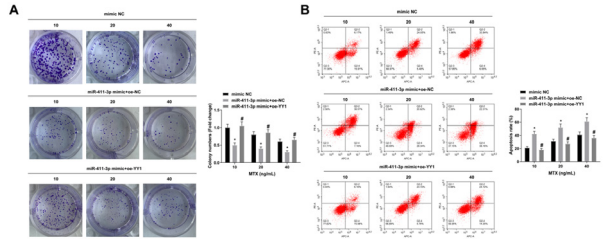

Figure 11. Elevation of YY1 could turn around elevating miR-411-3p's impacts on MTX cellular uptake and cytotoxicity in CEM-C1 cells.
(**A**) Clone formation assay detection of cell proliferation; (**B**) Flow cytometry detection of cell apoptosis; The data in the figures were all measurement data, and the values were clarified as mean ± S.D. (N=3); *vs. the mimic NC group, $P<0.05$, #vs. the miR-411-3p mimic+oe-NC, $P<0.05$.

MTX was clearly declined in CEM/CI cells transfected with oe-YY1 (Fig. 8B). It came out that after incubation with different concentrations of MTX, strengthening YY1 resulted in a clear decline in the repression rate of CEM/CI cells (Fig. 8C) and a distinct elevation in the number of colonies (Fig. 9A). It turned out that the apoptosis index of CEM/CI cells in the si-YY1 treated with different concentrations of MTX was declined at all MTX concentrations (Fig. 9B). Moreover, after incubation with different concentrations of MTX, depressing YY1 could motivate Bcl-2 but restrain Bax (Fig. 8DE). Overall, elevating YY1 can restrain MTX's cellular uptake and cytotoxicity, thereby motivating CEM/C1 cell growth.

Elevating YY1 turns around enhancive miR-411-3p's impacts on MTX's cellular uptake and cytotoxicity in CEM-C1 cells

To further explore miR-411-3p/YY1 axis' impacts on MTX's cellular uptake and cytotoxicity in CEM/C1 cells, it was transfected with mimic NC-miR-411-3p mimic+oe-YY1 or miR-411-3p mimic+oe-NC into CEM/C1 cells, and the successful transfection was verified (Fig. 10A). All results clarify that elevation of YY1 can turn around elevating miR-411-3p's impacts on MTX cellular uptake and cytotoxicity in CEM-C1 cells (Fig. 10B–E, Fig. 11A/B).

DISCUSSION

MTX is a chemotherapeutic drug for ALL's, which majorly exerts its therapeutic impact in ALL by impairing the synthesis of DNA in cells. The ability of leukemic blasts to uptake MTX and MTX-polyglutamate has been reported to be vital for the survival of children with ALL. However, MTX has a narrow therapeutic range, its pharmacokinetics and therapeutic response display great variability in ALL's, and it exhibits serious toxicity in plentiful patients, often resulting in an interruption or discontinuation of chemotherapy (Hu *et al.,* 2019). Recent studies have exhibited that miRNAs are implicated in the concentration of MTX in the blood of ALL patients (Wang *et al.,* 2014), suggesting that miRNAs are likely to participate in controlling the uptake of MTX by ALL cells. This research illustrated originally that elevation of miR-411-3p could motivate MTX's cellular uptake and cytotoxicity in CEM/C1 cells, and restrain cell growth, whereas repressing miR-411-3p did the opposite. Meanwhile, it was also testified that miR-411-3p functioned by targeting YY1.

Multiple studies have clarified that miR-411-3p takes part in various human diseases. For example, miR-411-3p was reduced in the tumor tissues of patients with multiple myeloma, and mediated LncRNA ANRIL dysregulation through hypoxia-inducible factor 1α to suppress the malignant proliferation and tumor growth of multiple myeloma stem cell-like properties (Wang *et al.,* 2020)]. (Fu *et al.,* 2020) testified that miR-411-3p was reduced in oral squamous cell carcinoma cells, and elevating miR-411-3p restrained cell growth by targeting NFAT5. miR-411-3p mitigated silica-induced pulmonary fibrosis (Gao *et al.,* 2020). Meanwhile, miR-411-3p was linked with the improved overall survival in lung cancer patients treated with nivolumab (Halvorsen *et al.,* 2018). However, miR-411-3p's impacts on the efficacy of MTX treatment in ALL patients are uncertain. In this research, elevation of miR-411-3p memorably enhanced MTX concentration, cell repression rate and apoptosis index, reduced colony number and suppressed Bcl-2 but motivated Bax in CEM/C1 cells treated with disparate concentrations of MTX, whereas depressing miR-411-3p had the exact opposite effect. These results conveyed that miR-411-3p could control MTX sensitivity in CEM/C1 cells.

YY1 is an extensively expressed multifunctional transcription factor affiliated with the GLI-Krüppel class of zinc finger proteins (Zhang *et al.,* 2021), which takes on momentous roles in diversified biological processes and is linked with tumorigenesis (Li *et al.,* 2020). discovered that YY1-mediated elevation of lncRNA MCM3AP-AS1 motivated lung cancer angiogenesis and progression(Chen *et al.,* 2019). confirmed that YY1 targeted tubulin polymerization-promoting protein and restrained pancreatic cancer migration, invasion, and angiogenesis through p38/MAPK and PI3K/AKT pathways (Li *et al.,* 2021). verified that YY1-induced elevation of LncRNA SNHG5 motivated angiogenesis in AML through the miR-26b/CTGF/VEGFA axis. Recently (Antonio-Andres *et al.,* 2021). confirmed that YY1 was elevated in peripheral blood leukemia cells of children with ALL with Pro-B and T phenotypes, and its elevation is clearly linked with poor survival. Meanwhile, YY1 has also been shown to be linked with drug resistance to multiple leukemia chemotherapeutics. For example (Zhang *et al.,* 2021). demonstrated that in chronic myeloid leukemia, KDM6A motivated imatinib resistance through YY1-mediated transcriptional elevation of TRKA. The present study discovered that repressing YY1 motivated MTX's cellular uptake and cytotoxic impacts, but repressed CEM/C1 cell growth, while enhancing YY1 turned around strengthening miR-411-3p's impacts on MTX cell uptake and cytotoxicity in CEM-C1 cells, and enhanced CEM/C1 cell growth.

However, this research still has several limitations. First, animal experiments were not performed to clarify miR-411-3p's impacts on MTX sensitivity. Secondly, it only figured out the regulatory effect of miR-411-3p on MTX sensitivity in a single ALL cell line (CEM/C1 cells) and not in other leukemia cell lines. Finally, further exploration of the downstream mechanisms of YY1 was not conducted. It is hoped that in future studies, the regulatory mechanism of miR-411-3p in leukemia MTX resistance can be further improved.

CONCLUSION

In short, this research demonstrated that miR-411-3p motivated MTX's cellular uptake and cytotoxic influences by targeting YY1 in ALL cells. The findings not only offer new insights into the mechanisms of variable MTX responses noticed in ALL patients, but also new references for addressing MTX chemotherapy resistance in ALL patients.

Declarations

Acknowledgments. Not applicable.

Availability of data and materials. The data are available from the corresponding author upon request.

Competing interests. The authors have no conflicts of interest to declare.

REFERENCES

Aberuyi N, Rahgozar S, Pourabutaleb E, Ghaedi K (2021) Selective dysregulation of ABC transporters in methotrexate-resistant leukemia T-cells can confer cross-resistance to cytarabine, vincristine and dexamethasone, but not doxorubicin. *Curr Res Transl Med* **69**: 103269. https://doi.org/10.1016/j.retram.2020.09.003

Ando Y, Shimada H, Matsumoto N, Hirota T, Oribe M, Otsuka E, Ishii K, Morimoto T, Ohashi K, Ieiri I (2013) Role of methotrexate polyglutamation and reduced folate carrier 1 (RFC1) gene polymorphisms in clinical assessment indexes. *Drug Metab Pharmacokinet* **28**: 442–445. https://doi.org/10.2133/dmpk.dmpk-12-rg-128

Antonio-Andres G, Jiménez-Hernandez E, Estrada-Abreo LA, Garfias-Gómez Y, Patino-Lopez G, Juarez-Mendez S, Huerta-Yepez S (2021) Expression of YY1 in pro-B and T phenotypes correlation with poor survival in pediatric acute lymphoblastic leukemia. *Pediatr Hematol Oncol* **38**: 456–470. https://doi.org/10.1080/08880018.2020.1871139

Chen Q, Yang C, Chen L, Zhang JJ, Ge WL, Yuan H, Meng LD, Huang XM, Shen P, Miao Y, Jiang KR (2019) YY1 targets tubulin polymerisation-promoting protein to inhibit migration, invasion and angiogenesis in pancreatic cancer *via* p38/MAPK and PI3K/AKT pathways. *Br J Cancer* **121**: 912–921. https://doi.org/10.1038/s41416-019-0604-5

de Beaumais TA, Jacqz-Aigrain E (2012) Intracellular disposition of methotrexate in acute lymphoblastic leukemia in children. *Curr Drug Metab* **13**: 822–834. https://doi.org/10.2174/138920012800840400

Fu SW, Zhang Y, Li S, Shi ZY, Zhao J, He QL (2020) LncRNA TTN-AS1 promotes the progression of oral squamous cell carcinoma *via* miR-411-3p/NFAT5 axis. *Cancer Cell Int* **20**: 415. https://doi.org/10.1186/s12935-020-01378-6

Gao X, Xu H, Xu D, Li S, Wei Z, Li S, Cai W, Mao N, Jin F, Li Y, Li T, Yi X, Liu H, Yang F (2020) MiR-411-3p alleviates Silica-induced pulmonary fibrosis by regulating Smurf2/TGF-β signaling. *Exp Cell Res* **388**: 111878. https://doi.org/10.1016/j.yexcr.2020.111878

Gervasini G, de Murillo SG, Jiménez M, de la Maya MD, Vagace JM (2017) Effect of polymorphisms in transporter genes on dosing, efficacy and toxicity of maintenance therapy in children with acute lymphoblastic leukemia. *Gene* **628**: 72–77. https://doi.org/10.1016/j.gene.2017.07.025

Halvorsen AR, Sandhu V, Sprauten M, Flote VG, Kure EH, Brustugun OT, Helland Å (2018) Circulating microRNAs associated with prolonged overall survival in lung cancer patients treated with nivolumab. *Acta Oncol* **57**: 1225–1231. https://doi.org/10.1080/0284186x.2018.1465585

Hu YH, Zhou L, Wang SS, Jing X, Guo HL, Sun F, Zhang Y, Chen F, Xu J, Ji X (2019) Methotrexate disposition in pediatric patients with acute lymphoblastic leukemia: what have we learnt from the genetic variants of drug transporters. *Curr Pharm Des* **25**: 627–634. https://doi.org/10.2174/1381612825666190329141003

Huang T, Chen Y, Zeng Y, Xu C, Huang J, Hu W, Chen X, Fu H (2021) Long non-coding RNA PSMA3-AS1 promotes glioma progression through modulating the miR-411-3p/HOXA10 pathway. *BMC Cancer* **21**: 844. https://doi.org/10.1186/s12885-021-08465-5

Iparraguirre L, Gutierrez-Camino A, Umerez M, Martin-Guerrero I, Astigarraga I, Navajas A, Sastre A, Garcia de Andoin N, Garcia-Orad A (2016) MiR-pharmacogenetics of methotrexate in childhood B-cell acute lymphoblastic leukemia. *Pharmacogenet Genomics* **26**: 517–525. https://doi.org/10.1097/fpc.0000000000000245

Jaramillo AC, Cloos J, Lemos C, Stam RW, Kaspers GJL, Jansen G, Peters GJ (2019) *Ex vivo* resistance in childhood acute lymphoblastic leukemia: Correlations between BCRP, MRP1, MRP4 and MRP5 ABC transporter expression and intracellular methotrexate polyglutamate accumulation. *Leuk Res* **79**: 45–51. https://doi.org/10.1016/j.leukres.2019.02.008

Li X, Yu M, Yang C (2020) YY1-mediated overexpression of long noncoding RNA MCM3AP-AS1 accelerates angiogenesis and progression in lung cancer by targeting miR-340-5p/KPNA4 axis. *J Cell Biochem* **121**: 2258–2267. https://doi.org/10.1002/jcb.29448

Li ZJ, Cheng J, Song Y, Li HH, Zheng JF (2021) LncRNA SNHG5 upregulation induced by YY1 contributes to angiogenesis *via* miR-26b/CTGF/VEGFA axis in acute myelogenous leukemia. *Lab Invest* **101**: 341–352. https://doi.org/10.1038/s41374-020-00519-9

Liang C, Li Y, Wang LN, Zhang XL, Luo JS, Peng CJ, Tang WY, Huang LB, Tang YL, Luo XQ (2021) Up-regulated miR-155 is associated with poor prognosis in childhood acute lymphoblastic leukemia and promotes cell proliferation targeting ZNF238. *Hematology* **26**: 16–25. https://doi.org/10.1080/16078454.2020.1860187

Lin C, Chen D, Xiao T, Lin D, Lin D, Lin L, Zhu H, Xu J, Huang W, Yang T (2021) DNA methylation-mediated silencing of microRNA-204 enhances T cell acute lymphoblastic leukemia by up-regulating MMP-2 and MMP-9 *via* NF-κB. *J Cell Mol Med* **25**: 2365–2376. https://doi.org/10.1111/jcmm.15896

Liu H, Ni Z, Shi L, Ma L, Zhao J (2019) MiR-486-5p inhibits the proliferation of leukemia cells and induces apoptosis through targeting FOXO1. *Mol Cell Probes* **44**: 37–43. https://doi.org/10.1016/j.mcp.2019.02.001

Liu J, Chen Z, Cui Y, Wei H, Zhu Z, Mao F, Wang Y, Liu Y (2020) Berberine promotes XIAP-mediated cells apoptosis by upregulation of miR-24-3p in acute lymphoblastic leukemia. *Aging (Albany NY)* **12**: 3298–3311. https://doi.org/10.18632/aging.102813

Naghizadeh S, Mohammadi A, Duijf PHG, Baradaran B, Safarzadeh E, Cho WC, Mansoori B (2020) The role of miR-34 in cancer drug resistance. *J Cell Physiol* **235**: 6424–6440. https://doi.org/10.1002/jcp.29640

Oosterom N, Berrevoets M, den Hoed MAH, Zolk O, Hoerning S, Pluijm SMF, Pieters R, de Jonge R, Tissing WJE, van den Heuvel-Eibrink MM, Heil SG (2018) The role of genetic polymorphisms in the thymidylate synthase (TYMS) gene in methotrexate-induced oral mucositis in children with acute lymphoblastic leukemia. *Pharmacogenet Genomics* **28**: 223–229. https://doi.org/10.1097/fpc.0000000000000352

Panetta JC, Sparreboom A, Pui CH, Relling MV, Evans WE (2010) Modeling mechanisms of *in vivo* variability in methotrexate accumulation and folate pathway inhibition in acute lymphoblastic leukemia cells. *PLoS Comput Biol* **6**: e1001019. https://doi.org/10.1371/journal.pcbi.1001019

Ranjbar R, Karimian A, Aghaie Fard A, Tourani M, Majidinia M, Jadidi-Niaragh F, Yousefi B (2019) The importance of miRNAs and epigenetics in acute lymphoblastic leukemia prognosis. *J Cell Physiol* **234**: 3216–3230. https://doi.org/10.1002/jcp.26510

Rushworth D, Mathews A, Alpert A, Cooper LJ (2015) Dihydrofolate reductase and thymidylate synthase transgenes resistant to methotrexate interact to permit novel transgene regulation. *J Biol Chem* **290**: 22970–22976. https://doi.org/10.1074/jbc.C115.671123

Wang LS, Li L, Li L, Chu S, Shiang KD, Li M, Sun HY, Xu J, Xiao FJ, Sun G, Rossi JJ, Ho Y, Bhatia R (2015) MicroRNA-486 regulates normal erythropoiesis and enhances growth and modulates drug response in CML progenitors. *Blood* **125**: 1302–1313. https://doi.org/10.1182/blood-2014-06-581926

Wang M, Zhao HY, Zhang JL, Wan DM, Li YM, Jiang ZX (2020) Dysregulation of LncRNA ANRIL mediated by miR-411-3p inhibits the malignant proliferation and tumor stem cell like property of multiple myeloma *via* hypoxia-inducible factor 1α. *Exp Cell Res* **396**: 112280. https://doi.org/10.1016/j.yexcr.2020.112280

Wang SM, Sun LL, Zeng WX, Wu WS, Zhang GL (2014) Effects of a microRNA binding site polymorphism in SLC19A1 on methotrexate concentrations in Chinese children with acute lymphoblastic leukemia. *Med Oncol* **31**: 62. https://doi.org/10.1007/s12032-014-0062-0

Wang SM, Zeng WX, Wu WS, Sun LL, Yan D (2017) Association between MTHFR microRNA binding site polymorphisms and methotrexate concentrations in Chinese pediatric patients with acute lymphoblastic leukemia. *J Gene Med* **19**: 353–359. https://doi.org/10.1002/jgm.2990

Wang Y, Huang Y, Liu H, Su D, Luo F, Zhou F (2019) Long noncoding RNA CDKN2B-AS1 interacts with miR-411-3p to regulate ovarian cancer *in vitro* and *in vivo* through HIF-1a/VEGF/P38 pathway. *Biochem Biophys Res Commun* **514**: 44–50. https://doi.org/10.1016/j.bbrc.2019.03.141

Wei J, Lu Y, Wang R, Xu X, Liu Q, He S, Pan H, Liu X, Yuan B, Ding Y, Zhang J (2021) MicroRNA-375: potential cancer suppressor and therapeutic drug. *Biosci Rep* **41**. https://doi.org/10.1042/bsr20211494

Woźniak M, Makuch S, Pastuch-Gawołek G, Wiśniewski J, Szeja W, Nowak M, Krawczyk M, Agrawal S (2021) The effect of a new glucose-methotrexate conjugate on acute lymphoblastic leukemia and non-hodgkin's lymphoma cell lines. *Molecules* **26**. https://doi.org/10.3390/molecules26092547

Wu F, Yin C, Qi J, Duan D, Jiang X, Yu J, Luo Z (2020) miR-362-5p promotes cell proliferation and cell cycle progression by targeting GAS7 in acute myeloid leukemia. *Hum Cell* **33**: 405–415. https://doi.org/10.1007/s13577-019-00319-4

Xian D, Zhao Y (2019) LncRNA KCNQ1OT1 enhanced the methotrexate resistance of colorectal cancer cells by regulating miR-760/PPP1R1B *via* the cAMP signalling pathway. *J Cell Mol Med* **23**: 3808–3823. https://doi.org/10.1111/jcmm.14071

Xu W, Li Z, Zhu X, Xu R, Xu Y (2018) miR-29 Family inhibits resistance to methotrexate and promotes cell apoptosis by targeting COL3A1 and MCL1 in osteosarcoma. *Med Sci Monit* **24**: 8812–8821. https://doi.org/10.12659/msm.911972

Zhang C, Shen L, Zhu Y, Xu R, Deng Z, Liu X, Ding Y, Wang C, Shi Y, Bei L, Wei D, Thorne RF, Zhang XD, Yu L, Chen S (2021) KDM6A promotes imatinib resistance through YY1-mediated transcriptional upregulation of TRKA independently of its demethylase activity in chronic myelogenous leukemia. *Theranostics* **11**: 2691–2705. https://doi.org/10.7150/thno.50571

Zhang L, Zou L, Sun P (2021) Relationship between miR-378c and YY1 expression in patients with gastric cancer and the clinicopathological features. *Cell Mol Biol Lett* **26**: 12. https://doi.org/10.1186/s11658-021-00256-x